Hydrodynamics from Landau initial conditions

2015 J. Phys.: Conf. Ser. 630 012042

(http://iopscience.iop.org/1742-6596/630/1/012042)

Journal of Physics: Conference Series **630** (2015) 012042 doi:10.1088/1742-6596/630/1/012042

Hydrodynamics from Landau initial conditions

Abhisek Sen[1],Jochen Gerhard[2],Giorgio Torrieri[3],Kenneth Read[4,1],Cheuk-Yin Wong[4]

[1]University of Tennessee, Knoxville, TN 37996
[2]Frankfurt Institute for Advanced Studies (FIAS), Frankfurt am Main, Germany
[3] IFGW, Universidade Estadual de Campinas, Campinas, São Paulo, Brazil
[4]Oak Ridge National Laboratory, Oak Ridge, TN 37831

E-mail: torrieri@ifi.unicamp.br

Abstract. We investigate ideal hydrodynamic evolution, with Landau initial conditions, both in a semi-analytical 1+1D approach and in a numerical code incorporating event-by-event variation with many events and transverse density inhomogeneities. The object of the calculation is to test how fast would a Landau initial condition transition to a commonly used boost-invariant expansion. We show that the transition to boost-invariant flow occurs too late for realistic setups, with corrections of $\mathcal{O}(20-30\%)$ expected at freezeout for most scenarios. Moreover, the deviation from boost-invariance is correlated with both transverse flow and elliptic flow, with the more highly transversely flowing regions also showing the most violation of boost invariance. Therefore, if longitudinal flow is not fully developed at the early stages of heavy ion collisions, 2+1 dimensional hydrodynamics is inadequate to extract transport coefficients of the quark-gluon plasma. Based on [1, 2]

1. Introduction

The quantitative modeling of matter produced in high energy heavy ion collisions with relativistic hydrodynamics is now a well-established field, following the widely cited announcement that matter produced at the relativistic heavy ion collider (RHIC), behaves as a "perfect fluid" [3]. The evidence for this behavior comes from the successful modeling of RHIC anisotropic flow by boost-invariant hydrodynamics. It is now clear that the same fluid-like behavior persists at the LHC [5, 6, 7]. It is commonly argued [8, 9, 10] that, given precise enough data on soft physics, chiefly momentum spectra and their azimuthal anisotropy, the transport coefficients of matter created in ultrarelativistic heavy ion collisions can be quantitatively constrained.

These models are all based on the reduction, either exact or approximate, of the problem to a 2+1 dimensional system [11], based on the symmetry of boost-invariance. Essentially, the system is assumed to have *as an initial condition* a longitudinal flow that is Hubble-like in the beam direction (usually associated with the "z" coordinate) *only*. This means that, initially,

$$v_z = \frac{z}{t}, \qquad y_s = y_f = \langle y \rangle_p , \tag{1}$$

where y_s and y_f are respectively the spacetime and flow rapidities

$$y_s = \frac{1}{2}\ln\left(\frac{t+z}{t-z}\right), \qquad y_f = \frac{1}{2}\ln\left(\frac{1+v_z}{1-v_z}\right),$$

$$\langle y \rangle_p = \frac{1}{2} \left\langle \ln \left(\frac{E + p_z}{E - p_z} \right) \right\rangle \simeq \frac{1}{2} \ln \cot \frac{p_z}{|p|}$$

with y_p being usually referred to as pseudo-rapidity. A further simplification comes from assuming that all initial dynamics does not depend on y

$$\frac{d}{dy} \frac{dN}{dy} = 0, \qquad \frac{dv_T}{dy} = 0 \tag{2}$$

or, equivalently not on t, z separately, but just on

$$\tau = \sqrt{t^2 - z^2} \tag{3}$$

(evolved from an initial time τ_0) and transverse degrees of freedom. An initial condition that respects Eq. (1) but not Eq. (2) will slowly degrade the constraints of Eq. (1), as shown in [12, 13, 14].

Initially, a different model has originally been advocated as the obvious initial state for the hydrodynamic evolution of the fluid: Landau hydrodynamics [15, 16, 19, 20]. In this picture, the energy that forms the bulk of the expanding fireball "stops" at midrapidity at time zero (in the collider frame). The initial distribution of matter is therefore a "pancake", of thickness 2Δ related to the boosted charge radius R of the nuclei with nucleon mass m_N at center of mass energy of $\sqrt{s_{NN}}$ where

$$\Delta \to \Delta_{lim} \simeq \frac{R}{\gamma} = \frac{R m_N}{(\sqrt{s_{NN}}/2)}. \tag{4}$$

In a more general implementation, Δ need not be defined by Eq. (4) and can be a free parameter, reflecting the spread in configuration space of low x gluons. The initial Landau condition is defined by the assumption that the initial "pancake" has no existing longitudinal flow at all, unless there are initial inhomogeneities which lead to a net momentum in local transverse space. (This is known as the "firestreak model" [21, 24]). Boost invariance is badly broken at the beginning of the fireball evolution and such a pancake has very little in common with the scenario used in [11, 13]. One can consider Bjorken and Landau as two extremes: In the Bjorken scenario, the nuclei originally pass through each other with minimal reinteraction and strings that stretch between colliding gluons arise in parallel to other strings. In the Landau scenario, they "stick together" or at least leave some energy in the middle.

While computationally reducing one dimension is highly desirable, a physics justification would be needed for the approximation of Eq. (1). A direct measurement of dN/dy is inconclusive. On the one hand, the Landau model fits a Gaussian well at all energies, with universal limiting fragmentation, as expected in [15, 16, 19]; moreover, strong violations of boost-invariance considerably lessen the HBT puzzle [25]. However, the *multiplicity* dependence on $\sqrt{s_{NN}}$ is not exactly that predicted in [15, 16, 19]. This by itself does not rule out the Landau scenario, as it can be accounted for by treating the initial thickness evolution with $\sqrt{s_{NN}}$ as a free parameter, as done in the Bjorken scenario.

There are two main arguments one can give for the Bjorken limit being more appropriate: The first one is that the perturbative partonic picture of the system [26, 27] makes this initial condition natural. However, even in the weakly-coupled limit, low x partons could lead to a breakdown of Eq. (2) (see for example, [28, 29]). Moreover, if the initial state is *strongly coupled* from the beginning, one could indeed expect that it would appear much more Landau-like [30, 31] than Bjorken-like, although the degree of stopping might also depend strongly on energy and system size [32, 33]. Stopping is therefore not determined *a priori*, as the interaction strength at the beginning of the system's evolution is currently a controversial topic.

The second reason is that, for mid-rapidity data, it is widely believed that the distinction between Bjorken and Landau evolution is irrelevant. As is clear from [15], Landau evolution

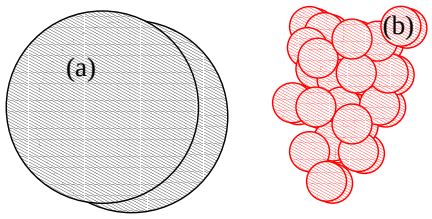

Figure 1. Landau initial condition (panel (a)), and actual Glauber initial conditions (panel (b)) for a typical event.

converges to Bjorken evolution after some sufficient time. The reason for this behavior is that longitudinal flow forms on the scale of $\sim \Delta/c_s$, while transverse flow forms on a much larger scale $\sim R/c_s$ where c_s is the speed of sound. Hence, since $\Delta \ll R$ for $\sqrt{s_{NN}} \gg 1$ GeV, initially the system can be considered, as indeed it is in [15], to be a purely 1D expanding "sharp step." As again shown in [15, 19, 20], the long-term longitudinal evolution of such a system at mid-rapidity is indistinguishable from that of [11]. Hence, 2+1 dimensional hydrodynamics can be safely used even if, at the very initial stage [13], the system is very far from boost invariance. Landau evolution at mid-rapidity can be treated as Bjorken with $\tau_0 \sim 1$ fm $\times$ GeV$/\sqrt{s_{NN}}$. Perhaps, this scaling will give unrealistically low initial proper times at the LHC, but since 2+1 simulations are only weakly sensitive to time, this might not be a fatal issue.

This idea, however, has two flaws: First of all, for a non-central collision, where anisotropic flow is most expected, locality and longitudinal momentum conservation imply that the system develops an additional initial longitudinal momentum imbalance, with extra longitudinal momentum due to the local (in transverse space) imbalance between the target and projectile $\rho^{P,T}_{part}(x_T) = d^2N^{P,T}_{part}/dx^2_T$ transverse participant density. Momentum conservation and the Landau condition (no transparency) constrain the initial $\gamma_z v_z$ to

$$\frac{v_z(x_T)}{\sqrt{1-v_z^2(x_T)}} = \frac{\rho^P_{part}(x_T) - \rho^T_{part}(x_T)}{\rho^P_{part}(x_T) + \rho^T_{part}(x_T)} K \tag{5}$$

K here is a free parameter, but it is clear that $K = \sqrt{s_{NN}}/m_N$ when $\Delta = \Delta_{lim}$ in Eq. (4). In general, $\Delta > \Delta_{\rm lim}$ reflects a picture where the partons carrying the dominant fraction of the nucleon's energy are parametrically much softer than the nucleon. This is equivalent to the "wee parton" picture, and implies they also carry less momentum. Assuming a linear dependence, the net momentum in an off-central collision is related to Δ by

$$K \simeq \frac{\sqrt{s_{NN}}}{m_N}\frac{\Delta_{lim}}{\Delta} = \frac{2R}{\Delta}. \tag{6}$$

This initial flow is trivially not boost invariant and it is not clear it disappears at *any* finite time for a general system evolving from a Landau initial condition.

Additionally, the "Landau→Bjorken" reasoning assumes that the longitudinal timescale is much larger than the transverse one. This is certainly true if the transverse scale is given as a radius of a homogeneous "pancake" of radius R given by an *average* of many events as in Fig. 1 (a). It is however less clear that such a hierarchy holds for a *typical* event as in Fig. 1(b). The inclusion of subnucleonic strong QCD fields [9] make this hierarchy even more dubious as the events with the strongest anisotropic coefficients would also have the most prominent "hotspots." Potentially, this effect makes the boost-invariant picture irrelevant *even for late-time hydrodynamics*: The more homogeneous regions will be more similar in their longitudinal

expansion to [11], while the more inhomogeneous regions would, on their own, evolve to a *3D Hubble* expansion [35]. The interplay between regions of different symmetry, and local instabilities [35, 36] makes any symmetry dubious.

In this work, we examine these issues systematically by both analytical and numerical methods. In the next section, we shall use a semi-analytical 1+1D calculation to examine the assumption that Landau hydrodynamics becomes bjorken-like. Then, we use a numerical code to investigate the role in initial-state anisotropies and transverse flow from a Landau initial condition.

2. Analytical calculation

2.1. The Khalatnikov solution

For the Landau initial condition of a reflectively symmetric slab of a relativistic hot, dense matter initially at rest, the Khalatnikov solution is an analytical solution of the hydrodynamical equation that describes the space-time evolution of the system. The solution is obtained by introducing a hydrodynamical potential χ that is a function of the hydrodynamical variables of the energy density field ϵ and the velocity field v, which can be alternatively represented by the energy density logarithm y and the flow rapidity α,

$$\epsilon/\epsilon_0 = (s/s_0)^{4/3} = (T/T_0)^4 = e^{4y}, v = \tanh\alpha, \tag{7}$$

where ϵ_0 is the initial energy density and the flow rapidity α is also represented by the symbol y_f. The Khalatnikov solution consists of writing the space-time coordinates (z,t) as functions of the hydrodynamical variables (y,α), given in Eq. (4.30)-(4.12a) of Ref. [18], as

$$t(y,\alpha) = e^{-y}\left(\frac{\partial\chi}{\partial y}\cosh\alpha - \frac{\partial\chi}{\partial\alpha}\sinh\alpha\right), \tag{8}$$

$$x(y,\alpha) = e^{-y}\left(\frac{\partial\chi}{\partial y}\sinh\alpha - \frac{\partial\chi}{\partial\alpha}\cosh\alpha\right). \tag{9}$$

Belenkij and Landau considered the initial slab of width $2l$ and chose the origin of the longitudinal z-coordinate at $x{=}{-}l$. The longitudinal coordinates z is therefore related to the quantity x in Eq. (9) by $z = x + l$. As we are considering a system possessing a reflection symmetry with respect to $z = 0$, we need to examine only the region of $z \geq 0$.

The Khalatnikov solution is uniquely specified by the requirement to satisfy two boundary conditions: (i) zero velocity ($v{=}0$ and $\alpha{=}0$) at the center of the symmetric slab at $z{=}0$ (and $x{=}{-}l$), and (ii) the matching to the Riemann simple wave solution when $y{=}{-}\alpha c_s$ at the boundary of the slab. It is given in terms of the hydrodynamic potential $\chi(y,\alpha)$ in Eq. (4.30) of [18] by

$$\chi(y,\alpha) = -l\sqrt{3}e^{y}\int_{\alpha/\sqrt{3}}^{-y} e^{2y'} I_0\left[\sqrt{y'^2 - \frac{1}{3}\alpha^2}\right] dy' \tag{10}$$

The above solution (10) has been obtained for the ideal equation of state, $p = e/3$ with speed of sound $1/\sqrt{3}$.

In the Khalatnikov solution, there are two hydrodynamical degrees of freedom which have been chosen to be the energy density ϵ and the velocity field v or alternately (y,α). There is however another Riemann wave simple wave solution of the one-dimensional relativistic hydrodynamical equations in which the energy density field represented by y and the velocity field represented by α can be expressed as a function of each other in which the space-time coordinates x and t do not explicitly appear. In the presence of a disturbance, the simple wave propagation can be visualized as the superposition of (i) the propagation of a sound wave

with the speed of sound c_s and (ii) the propagation of the fluid element itself with a flow velocity $v = \tanh\alpha$. They occur at the boundary regions where the energy density decreases monotonically until the energy density vanishes when the matter is in contact with the vacuum. As the two boundaries of the slab are always in contact with the vacuum, the Riemann simple wave solution are always present on these slab boundaries.

Because of this mutual dependencies between y and α for the Riemann simple wave, there is then only a single independent hydrodynamical degree of freedom in the Riemann simple wave solution. The hydrodynamics is described by $y(\alpha(x,t))$ or vice-versa $\alpha(y(x,t))$ in the form of a running wave whose profile can change with time. In relativistic hydrodynamics, this becomes [23]:

$$\alpha = \tanh^{-1} v \quad = \quad \pm \int \frac{c_s d\epsilon}{(\epsilon + p)} = \pm \frac{c_s}{c_s^2} \ln(\epsilon/\epsilon_0)^{1/4},$$

which leads to $\alpha = -\ln(T/T_0)/c_s$, with the sign chosen since energy density decreases with time.

In terms of the potential χ in Eqs. (8) and (9), we have

$$\frac{x}{t} \quad = \quad \frac{\tanh\alpha - \frac{\partial\chi}{\partial\alpha}/\frac{\partial\chi}{\partial y}}{1 - \tanh\alpha \;\; (\frac{\partial\chi}{\partial\alpha}/\frac{\partial\chi}{\partial y})} = \frac{\tanh(-y/c_s) - c_s}{1 - \tanh(-y/c_s)c_s}. \tag{11}$$

since or simple waves with a center at the origin, the total derivative of the potential function $\chi(y,\alpha)$ is zero [23].

After the time $t \geq l/c_s$, the rarefaction wave that starts from the edge of the slab at $z=l$ reaches the center of the slab at $z=0$ (Fig. 1). Subsequent expansion of the fluid in the central region will proceed through the Khalatnikov solution of Eqs. (8), (9), and (10). From Equation 10 we get, after some algebra

$$\frac{\partial\chi}{\partial\alpha}(y,\alpha) \quad = \quad l(\alpha/\sqrt{3})e^y \int_{\alpha/\sqrt{3}}^{-y} e^{2y'} \frac{I_1\left[\sqrt{y'^2 - \frac{1}{3}\alpha^2}\right]}{\sqrt{y'^2 - \frac{1}{3}\alpha^2}} dy' + l e^y e^{2\alpha/\sqrt{3}}. \tag{12}$$

With the knowledge of $\partial\chi/\partial y$ and $\partial\chi/\partial\alpha$ given by Eq. (12), the right-hand sides of Eqs. (8) and (9) give (x,t) as explicit functions of (y,α). The integral in Eq. (12) can be evaluated numerically as the limits of the integration and the integrands are known functions of y and α.

Not all portions of the Khalatnikov solution shown as the solid curves can be used to describe the evolution of the system as the dynamics at the edge is described by the propagation of a disturbance arising from the presence of the edge boundary, and the accompanying hydrodynamical motion is a simple wave propagating from the edge toward the center. The solution at the edge of the slab is governed by the Riemann simple wave solution. The Khalatnikov solution that is applicable in the interior of the slab needs to be matched with the simple wave solution when the energy density logarithm y matches the rapidity α with $\alpha = -y/c_s$.

We can carry out the matching in the following way. We study the hydrodynamical solution for a fixed value of t ($\geq l/c_s$) and increase stepwise the value of α, starting from $\alpha=0$. We calculate y and z as a function of t and α. After determining y for the pair of (t,α) values, we test whether $-\sqrt{3}y$ remains greater than α or not. If $-\sqrt{3}y$ remains greater than α, we proceed to the next incremented value of α and look for the Khalatnikov solution for the next set of (t,α) pair. On the other hand, when $-\sqrt{3}y$ is equal to or just begin to be greater than α, the solution will be switched to the Riemann simple wave solutions for subsequent α values. In the simple wave boundary region for a fixed value of t, we increase stepwise the value of α and the energy density logarithm variable y is given by $y = -c_s\alpha$. Knowing and the values of t, α and

y, the spatial coordinate x is given by Eq. (11). This stepwise increase of α allows us to trace the energy density as a function of the longitudinal coordinates, for a fixed value of t.

The space-time coordinates (x,t) or (t,z) can be represented alternatively by the proper-time τ and spatial rapidity y_s given by Eq. 1 and Eq. 3 The initial simple wave propagation cannot be adequately represented in terms of real τ and y_s because $t \leq z$ for the initial slab. Real proper time and spatial rapidity commence at $t = l/c_s$ at the proper time of $\tau = l/c_s$, at which the rarefaction wave reaches the center of the slab and the Khalatnikov solution begin to come into play.

We need to express the Khalatnikov solution and the Riemann wave solution in terms of the proper time τ and spatial rapidity y_s. The Khalatnikov solution are given by Eq. (23) where t and x are expressed as functions of y and α by Eqs. (8), (9), with the hydrodynamical potential χ determined by Eq. (10). With the knowledge of $\partial\chi/\partial y$ and $\partial\chi/\partial\alpha$ given by Eq. (12) the (τ, y_s) variables are explicit functions of (y,α).

In terms of the (τ, y_s) coordinates, the Riemann simple wave solution can be obtained by considering the effective velocity a as

$$a = \frac{v - c_s}{1 - vc_s}. \tag{13}$$

The simple wave solution in terms of (τ, y_s) becomes

$$e^{y_s} = \frac{1 + \sqrt{1 + (\tau/l)^2(1-a^2)}}{(\tau/l)(1-a)}, \tag{14}$$

which describes the hydrodynamical motion of disturbances in the boundary regions of the slab. The Khalatnikov solution needs to match to the Riemann wave solution when the energy logarithm y and the rapidity α is related by the speed of sound, $y = -\alpha c_s$.

We consider a fixed value of $\tau \geq l/c_s$ and stepwise increase the value of α, starting from α=0. We can obtain the hydrodynamical description of (y,α) as a function of (τ, y_s) by inverting Eq. (3,2). For each pair of (τ,α) values, Eq. (3) with supplementary equations (8) and (9) presents itself as an equation for the unknown quantity y. We can solve this equation with only one unknown numerically. After the solution of y is obtained, Eqs. (12) and (12) are then used with Eq. (9) to calculate the value of x, z and y_s. The newly determined y can be used as the trail value for the next α to get the new solution of y.

Using the method we have just outlined for $\tau \geq l/c_s$, we can determine the Khalatnikov solution as a function of the spatial rapidity y_s for a fixed value of τ shown as solid curves in Fig. 4. However, it is necessary to match the Khalatnikov solution to the Riemann simple wave when y is equal to $-\alpha c_s$. Starting from $y_s = 0$ at $\alpha = 0$, we can carry out the simple wave matching by testing $-y$ against $c_s\alpha$. When $-y$ is equal to or just begin to be greater than $c_s\alpha$, the solution will be switched to simple wave solutions for subsequent α values. For the simple wave solution at a fixed value of τ, the energy density logarithm variable y is given by $y = -c_s\alpha$ and the spatial rapidity y_s is given by Eq. (14). The hydrodynamical solution with properly matched Khalatnikov solution and Riemann simple waves are shown as the dashed curves in Fig. 4. They are the hydrodynamical solutions satisfying the boundary conditions.

We show in Fig. 5 the dynamics of the system for later times of τ = 10 30, 50, and 70 l. The energy density is relatively flat but the flow rapidity α is slightly greater than the spatial rapidity y_s.

The solution of (y,α) as a function of (t,z) or (τ, y_s) allows one to extract other hydrodynamical quantity of interest. In addition to the energy density, one can calculate the spatial profiles of the temperature or entropy density at different times t or proper times τ.

In Fig. 8, we show the ratio ϵ/ϵ_0 at the center of the slab at $z = 0$ as a function of the proper time τ/l. The energy density decreases with τ/l but the decrease does not follow the Bjorken

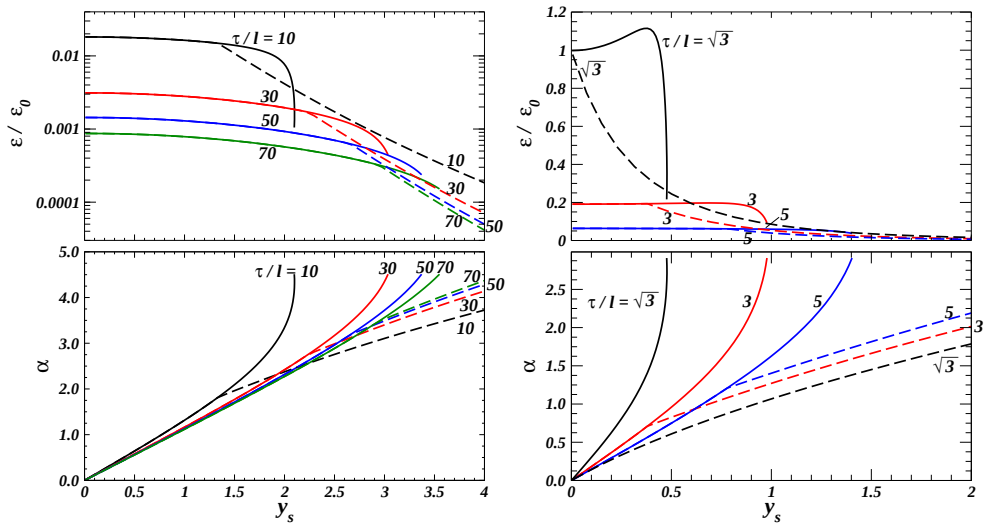

Figure 2. (Color online) right panel: The quantities $(\epsilon/\epsilon_0, \alpha)$ as a function of the spatial rapidity y_s for different values of τ/l. Left panel: The quantities $(\epsilon/\epsilon_0, \alpha)$ as a function of the spatial rapidity y_s for different values of τ/l. In both cases The solid curves give the Khalatnikov solutions which must be matched on to Riemann simple wave solutions shown as dashed curves.

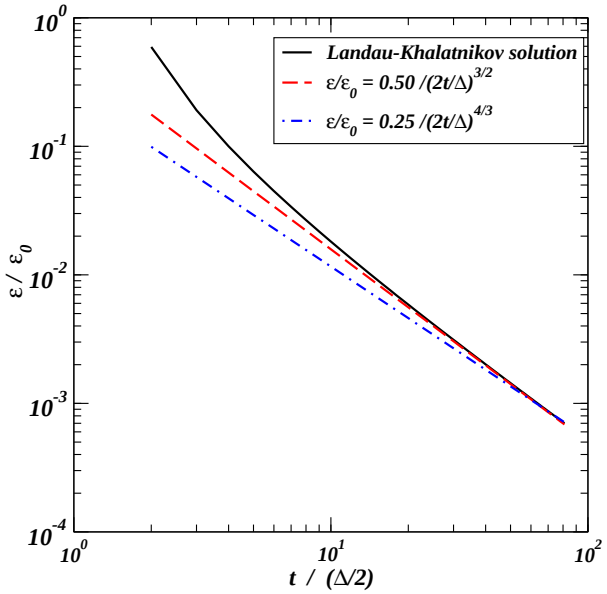

Figure 3. (Color online) The ratio ϵ/ϵ_0 at $z = 0$ as a function of τ/l. The solid curves represent the solutions from the Khalatnikov solution with the Landau initial condition, and the dashed curve is the behavior expected from Bjorken hydrodynamics.

limit of $\epsilon/\epsilon \propto 1/\tau^{4/3}$. Bjorken-like behavior of $\epsilon \propto 1/\tau^{4/3}$ behavior occurs only at the very late stage of $\tau/l \sim 80$, useless for any phenomenological study.

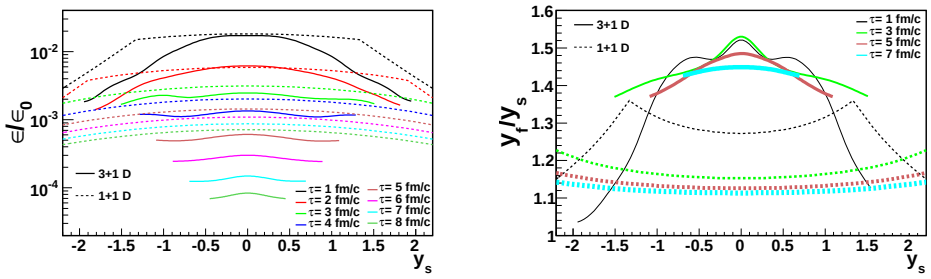

Figure 4. (color online) Left panel: Ratio of energy density at the indicated time to the initial energy density as a function of rapidity. The dashed lines show the analytical solution [22] while the solid lines show the numerical calculation, including net momentum, transverse expansion and inhomogeneities. Right panel: The y_f/y_s ratio (solid lines) as a function of proper time and rapidity, averaged over all events, at $r_\perp = 0$. The analytical 1D solution [22] is also plotted (dashed lines).

3. Numerical calculation

The Glauber Monte Carlo description of two colliding Au^{197} nuclei at 200 GeV was used to generate the initial condition relevant to RHIC. Nucleons were distributed as per a Wood-Saxon distribution with radius 6.38 fm, and diffuseness 0.535 fm. The impact parameters were simulated randomly following a distribution of $d\sigma/db = 2\pi b$. The nucleons were assumed to have no hard-core and the condition for nucleon-nucleon collision is that the inter-nucleon distance d should satisfy $\pi d^2 < \sigma_{NN}$, where $\sigma_{NN} = 42$ mb is the nucleon-nucleon cross section.

We then use the CL-SHASTA code developed in [37] to evolve this configuration according to ideal hydrodynamics, $\partial_\mu T^{\mu\nu} = 0$ with

$$T_{\mu\nu} = (\rho + p)u_\mu u_\nu + p g_{\mu\nu} \tag{15}$$

$$u_\mu = \frac{1}{\sqrt{1 - v_z^2 - v_T^2}} (1, v_T \sin(\theta), v_T \cos(\theta), v_z) \tag{16}$$

where $v_z = \tanh y_L$. With an ideal gas equation of state, $p = \rho/3, c_s = 1/\sqrt{3}$, and $\Delta = 0.1$ fm, and longitudinal flow given by Eq. (5). Our results do not qualitatively change if the longitudinal thickness if changed by $\mathcal{O}(50 - 100\%)$.

The high-statistics 3D calculations were performed at the Oak Ridge National Laboratory using the code in [37].

After simulating 10000 events for a given configuration and initial conditions, each of which evolves the millions of grid cells over 300 small time steps in the lab frame covering an expansion until 10 fm/c, we divide them into spacetime rapidity slices. The energy density evolution as a function of spacetime rapidity is shown in Fig. 4 left panel, which follows the trend in [15] to ∼20% precision, as expected from correction due to transverse and elliptic flow. Hence, the left panel of Fig. 4 show a decreasing bump in e (which correlates with transverse multiplicity$dN/dy \sim S\tau_0 e^{3/4}$ and transverse energy $dE_T/dy \sim S\tau_0 e$ in the Bjorken picture [11]. Here $S \sim R^2 \sim N_{part}^{2/3}$ is the transverse overlap area), making these similar to boost-invariant results [11]. Self-quenching variables (v_2, and to a lesser extent the average transverse momentum $\langle p_T \rangle$), however, will show such rapidity dependence independently of freezeout.

We then calculate the longitudinal flow rapidity y_f as well as the transverse flow for each slice of rapidity, averaged over the entire transverse volume, to explore boost invariance. Fig. 4 right

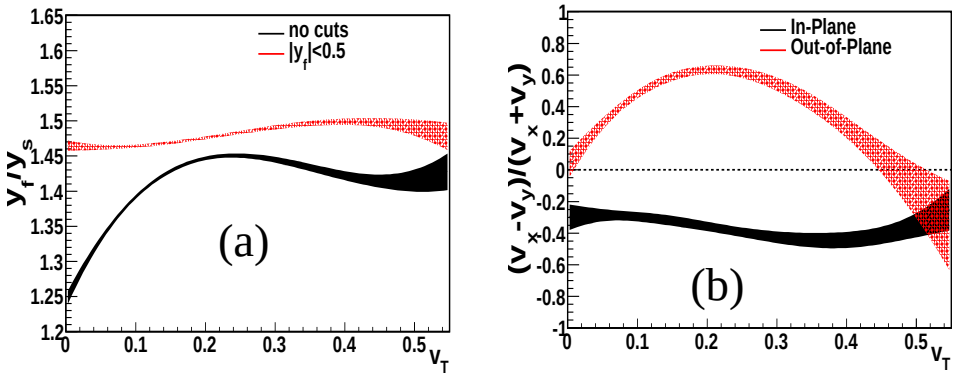

Figure 5. (color online) Panel (a) y_f/y_s as a function of mean transverse velocity for $|y_f| < 0.5$ (hashed red) and with no restriction on y_f (solid black). Panel (b) Distribution of transverse flow anisotropy versus mean total transverse velocity for in-plane (solid black) and out-of-plane (hashed red) flow. Both are averaged over fireball volume and event sample, with the bands representing the variance over the average across events.

panel shows the ratio y_f/y_s as a function of y_s at various relevant times in the evolution. If the system were exactly boost invariant, y_f/y_s would be strictly unity. As expected, the ratio does evolve towards unity as the system cools; however, it would be a gross oversimplification to treat the ratio as a constant or unity, even at significantly later times. At freezeout provided initial temperature $\simeq 300$ MeV, we predict y_f/y_s to be above unity by about 40% around midrapidity. At earlier stages, relevant for the formation of transverse and elliptic flow ($t \sim \epsilon R/c_s$), these corrections are of order 50%. For comparison, we superimpose the same distributions for the 1D expansion calculated in an analytical work [22]. It can be seen that, unlike what was presumed in [16, 19], transverse expansion and local dynamics make a qualitative, and not just a quantitative effect: deviation from boost invariance oscillates and stays nearly constant rather than decreases in time when transverse expansion and anisotropies are taken into account.

The relevance of this dynamics for transverse degrees of freedom is elucidated in Fig. 5, which shows the dependence of y_f/y_s, an indicator of the degree of violation of boost invariance, on transverse flow. Thus, if the Landau initial condition is more appropriate, transverse flow and its azimuthal anisotropies form, to a certain extent, in strongly non-boost invariant regions. This is readily understood, as such regions are precisely the places where transverse gradients are larger w.r.t. longitudinal ones. Hotspots can also have a non-zero longitudinal momentum and vorticity [17] (the "firestreak"), further invalidating local boost-invariance. As Fig. 5 panel (a) however shows, this result somewhat depends on the rapidity region being explored. A restriction in flow rapidity, approximately tracking the pseudorapidity, will ensure v_T is independent of the degree of boost invariance. Such a cut, however, does nothing to make the evolution examined more boost-invariant, since y_f/y_s remains very well away from unity.

Fig. 5 panel (b) shows the anisotropy of the in-plane and out of plane flow, as a function of transverse flow. This plot indicates that dynamics relevant for transverse and anisotropic flow significantly violates boost invariance if Landau initial conditions are assumed.

The viability of the computations performed here depends, of course, in the longitudinal structure of the event really being close to the Landau limit. Because we do not know this from first principles, and given the many undetermined parameters in a typical hydrodynamic simulation, we suggest that experimental tests specifically probing boost invariance should be

performed.

In conclusion, we have shown that, provided the system is Landau-like in its initial stages, it will not, as commonly expected, evolve to a Bjorken-like stage within realistic timescales. Furthermore, the deviation from boost invariance is directly correlated with the development of transverse and elliptic flow, the characteristic signatures used to demonstrate and quantitatively study the hydrodynamics of the quark-gluon plasma. In view of these results, the transport properties of the medium created in heavy ion collisions could be considerably different from those usually assumed.

This research used resources of the Oak Ridge Leadership Computing Facility at the Oak Ridge National Laboratory, which is supported by the Office of Science of the U.S. Department of Energy under Contract No. DE-AC05-00OR22725. We wish to thank Sean Gavin and Peter Steinberg for useful discussions.

[1] A. Sen, J. Gerhard, G. Torrieri, K. Read and C. Y. Wong, arXiv:1403.7990 [nucl-th].
[2] C. Y. Wong, A. Sen, J. Gerhard, G. Torrieri and K. Read, arXiv:1408.3343 [nucl-th].
[3] M. Gyulassy and L. McLerran, Nucl. Phys. A **750**, 30 (2005).
[4] E. Shuryak, Prog. Part. Nucl. Phys. **53**, 273 (2004).
[5] K. Aamodt *et al.* [ALICE Collaboration], Phys. Rev. Lett. **105**, 252302 (2010).
[6] S. Chatrchyan *et al.* [CMS Collaboration], Phys. Rev. C **87**, 014902 (2013).
[7] G. Aad *et al.* [ATLAS Collaboration], Phys. Rev. C **86**, 014907 (2012).
[8] H. Song, S. A. Bass and U. Heinz, Phys. Rev. C **83**, 054912 (2011) [Erratum-ibid. C **87**, 019902 (2013)].
[9] C. Gale, S. Jeon, B. Schenke, P. Tribedy and R. Venugopalan, Nucl. Phys. A904-905 **2013**, 409c (2013).
[10] R. A. Soltz, I. Garishvili, M. Cheng, B. Abelev, A. Glenn, J. Newby, L. A. Linden Levy and S. Pratt, Phys. Rev. C **87**, 044901 (2013).
[11] J. D. Bjorken, Phys. Rev. D **27**, 140 (1983).
[12] L. M. Satarov, A. V. Merdeev, I. N. Mishustin and H. Stoecker, Phys. Rev. C **75**, 024903 (2007).
[13] P. Bozek, Phys. Rev. C **77**, 034911 (2008).
[14] G. S. Denicol, T. Koide, P. Mota and T. Kodama, J. Phys. G **35**, 104130 (2008).
[15] L. D. Landau, Izv. Akad. Nauk Ser. Fiz. **17**, 51 (1953).
[16] P. Steinberg, Acta Phys. Hung. A **24**, 51 (2005) [nucl-ex/0405022].
[17] B. Betz, M. Gyulassy and G. Torrieri, Phys. Rev. C **76**, 044901 (2007) [arXiv:0708.0035 [nucl-th]].
[18] S. Z. Belenkij and L. D. Landau, Nuovo Cimento, Suppl. **3**, 15 (1956).
[19] C. -Y. Wong, EPJ Web Conf. **7**, 01006 (2010).
[20] C. -Y. Wong, Phys. Rev. C **78**, 054902 (2008).
[21] J. Gosset, J. I. Kapusta and G. D. Westfall, Phys. Rev. C **18**, 844 (1978).
[22] C.Y. Wong, A. Sen, J. Gerhard, G. Torrieri, and K.F. Read C. Y. Wong, A. Sen, J. Gerhard, G. Torrieri and K. Read, arXiv:1408.3343 [nucl-th].
[23] L. D. Landau and E. M. Lifshitz, *Fluid mechanics*, Pergamon Press, 1958.
[24] L.Cserai, Introduction to Relativistic Heavy Ion Collisions.
[25] M. Gyulassy and D. H. Rischke, Heavy Ion Phys. **17**, 261 (2003).
[26] R. P. Feynman, Phys. Rev. Lett. **23**, 1415 (1969).
[27] S. J. Brodsky, J. F. Gunion and J. H. Kuhn, Phys. Rev. Lett. **39**, 1120 (1977).
[28] W. Busza, Nucl. Phys. A **854**, 57 (2011).
[29] A. Capella, U. Sukhatme, C-ITan and J. Tran Thanh Van, Phys. Rept. **236**, 225 (1994).
[30] J. L. Albacete, Y. V. Kovchegov and A. Taliotis, JHEP **0905**, 060 (2009).
[31] D. Grumiller and P. Romatschke, JHEP **0808**, 027 (2008).
[32] J. Casalderrey-Solana, M. P. Heller, D. Mateos and W. van der Schee, Phys. Rev. Lett. **111**, 181601 (2013) [arXiv:1305.4919 [hep-th]].
[33] J. Casalderrey-Solana, M. P. Heller, D. Mateos and W. van der Schee, Phys. Rev. Lett. **112**, 221602 (2014) [arXiv:1312.2956 [hep-th]].
[34] C.E. Coleman-Smith and B. Müller, Phys. Rev. D **89**, 025019 (2014).
[35] H. Kouno, M. Maruyama, F. Takagi and K. Saito, Phys. Rev. D **41**, 2903 (1990).
[36] G. Torrieri and I. Mishustin, Phys. Rev. C **78**, 021901 (2008).
[37] J. Gerhard, V. Lindenstruth and M. Bleicher, Comput. Phys. Commun. **184**, 311 (2013).